Journal of Power Sources 255 (2014) 179–186

Contents lists available at ScienceDirect

Journal of Power Sources

journal homepage: www.elsevier.com/locate/jpowsour

The effect of fuel type on the performance of a direct carbon fuel cell with molten alkaline electrolyte

A. Kacprzak*, R. Kobyłecki*, R. Włodarczyk, Z. Bis

Department of Energy Engineering, Faculty of Environmental Engineering and Biotechnology, Czestochowa University of Technology, ul. Brzeźnicka 60a, 42-200 Częstochowa, Poland

HIGHLIGHTS

- The effect of nine carbonacious fuels on the operation of a DCFC was investigated.
- The tests were performed at 723 K and the air flow rate of 0.5 dm^3 min^{-1}.
- Binary eutectic mixture of Na/Li hydroxides was used as electrolyte.
- The results for a biochar fuel were similar to those obtained for hard coals.

ARTICLE INFO

Article history:
Received 20 June 2013
Received in revised form
12 December 2013
Accepted 4 January 2014
Available online 10 January 2014

Keywords:
Direct carbon fuel cell
Biochar
Coal
Carbon black
Molten hydroxide electrolyte
Anode

ABSTRACT

In the paper the behavior of various carbon-rich materials used as fuels for the direct carbon fuel cell (DCFC) with molten hydroxide electrolyte is presented. For the current research various carbonaceous fuels (e.g., different biochars, hard coal, graphite, carbon black) were tested. The electrolyte was the binary eutectic mixture of sodium and lithium hydroxides (90 mol.% NaOH – 10 mol.% LiOH). The fuel cell was operated at 723 K and cathode air flow rate of 0.5 dm^3 min^{-1}. The maximum power densities were achieved for raw coal and commercial biochar and made up 38.6 mW cm^{-2} and 32.8 mW cm^{-2}, respectively.

1. Introduction

The increase of human population, as well as the rapid economic growth and development require safe, trustable, and continuous supply of electricity. Despite the current policy and political situation focused on the promotion of energy conversion from renewable sources [1,2], still the majority of electricity roughly 67% is generated from non-renewables, such as coal (41%), crude oil (4%), or natural gas (22%) [3]. In some countries, e.g., Poland, China, South Africa, or Australia, coal is still the dominant fuel for electricity generation in domestic power plants [3,4].

Since the burning of coal and electricity generation in conventional power plants is often associated with quite low efficiency (30–45%) and brings about significant emissions of pollutants (SO_2, NO_x, particulates, as well as CO_2), numerous attempts have been made to search for new highly-efficient and low emission technologies of electricity generation [5]. One of the promising approaches to improve the efficiency of energy conversion from coal is the use of fuel cells, such as e.g., the Direct Carbon Fuel Cell (DCFC). The schematic of the DCFC operation is shown in Fig. 1. In the DCFC system the electrochemical reaction between the elemental carbon and oxygen is the source of electrons which pass through the external circuit and generate electricity.

This technology may significantly reduce the energy losses by direct conversion of solid carbon chemical energy into electricity [6]. The DCFC technology has been under investigation for several decades but, so far, has received less attention than fuel cell technologies focused on the use of hydrogen or natural gas. However, the DCFCs have two significant advantages over other fuel cells, since 1) their thermodynamic efficiency may theoretically exceed 100% i.e., much higher than that of e.g., hydrogen fuel cells where

* Corresponding authors. Tel.: +48 34 325 7334x18.
E-mail addresses: akacprzak@is.pcz.czest.pl (A. Kacprzak), rafalk@is.pcz.czest.pl (R. Kobyłecki).

0378-7753/$ – see front matter © 2014 Elsevier B.V. All rights reserved.
http://dx.doi.org/10.1016/j.jpowsour.2014.01.012

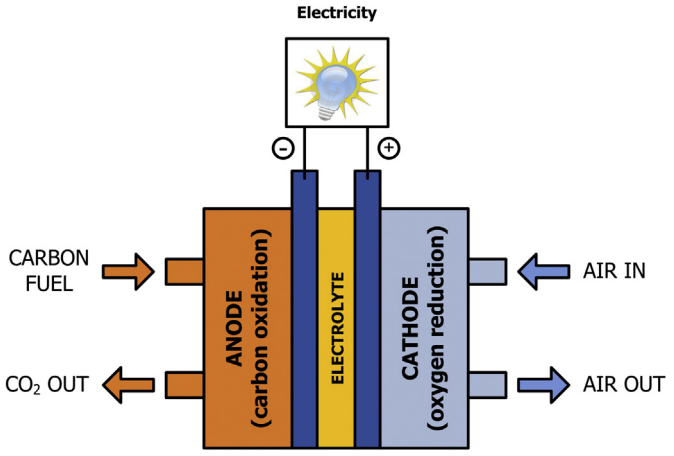

Fig. 1. The schematic of DCFC operation.

the efficiencies of roughly 83% have been reported [7], and 2) the DCFC may be fueled with any carbonaceous and solid (and thus easy to transport and store) fuel, such as e.g., hard coal, lignite, petcoke, biomass, or even carbonized waste [8]. Although the thermodynamic efficiency of the DCFC (η_{th}) calculated by Eq. (1). may theoretically exceed 100% since the oxidation of elemental carbon into gaseous CO_2 is accompanied by almost no entropy change ($\Delta S = 1.6\ J\ K^{-1}\ mol^{-1}$ at 873 K) practical operational efficiencies of the cells are lower and estimated at roughly 80% [6].

$$\eta_{th} = 1 - \frac{T\Delta S}{\Delta H} = \frac{\Delta G_{700K}}{\Delta H_{700K}} = \frac{-395.4\left[kJmol^{-1}\right]}{-394.0\left[kJmol^{-1}\right]} = 1.003 \qquad (1)$$

So far, three different electrolyte concepts (molten hydroxide, molten carbonate or solid oxygen ion conducting ceramic) have been proposed for the DCFC technology [8]. Although, there are several papers on the DCFC issue the number of publications where the authors focus on the investigation of the DCFCs operation with aqueous hydroxide or molten hydroxide electrolytes is quite limited [9–12]. The results reported by Nunoura et al. [12] indicated that aqueous electrolyte provided the conditions for low-temperature operation of the cell (423–523 K) and thus the possibility to use cheaper materials for the cell body. Nunoura et al. [12] used a corncob biochar fueled cell with potassium and lithium hydroxide mixture electrolyte operated at 518 K and 35.8 bar pressure but reported the maximum power density of only 6.5 mW cm^{-2}.

In order to improve the cell performance and electricity yield the molten hydroxides are required. Zecevic et al. [9,10] in cooperation with the West Virginia University [11] reported stable performance of the cell, and the power density of 58 mW cm^{-2} for MARK III-A prototype. Unfortunately, they only focused on the use of some specially prepared carbon rods of graphite and coal origin, and tested no granulates.

Since except for just a few cases [13,14] there has been no information so far, on the experiments where the authors would investigate the possibility to operate the DCFC with minimum fuel preparation (e.g., no rods manufacturing) and with granulate carbonaceous fuels, particularly of biomass origin, the intention of this paper is to provide some experimental data on that issue and report the results of a DCFC operated with various granulate carbonatious fuels, such as biomass-derived biochars, hard coals, carbon black, and graphite.

2. Experimental

2.1. Fuel samples

Nine types of various carbonaceous fuels, i.e., commercial graphite, carbon black (type N220, Konimpex), two types of commercial hard coal and five types of biochar were used for the present investigation. Four of the fuels were produced by the authors from the carbonization of various biomass types (apple tree chips, sunflower husks, pine and energetic willow shavings) while the fifth sample was a commercial biochar. In order to produce the biochars from the 'raw' fuels the biomass samples were crushed, then sieved (particle size <0.5 mm), and finally charred at 873 K for 30 min. The details of the carbonization technology were described elsewhere [15,16].

All fuel samples were analyzed according to Polish standards with respect to their ultimate and proximate analysis. The ultimate analysis was conducted with the use of Leco TruSpec CHNS analyzer, while automatic isoperibol calorimeter (IKA C2000 Basic) was used to determine the higher heating values (HHV) of all the samples. Mercury intrusion porosimeter (Poremaster 33, Quantachrome) was used to determine total surface area and pore volume of the samples, as well as to investigate their pore size distributions. The data provided by the porosimetry is important since those parameters are directly related to the wet-ability, electrochemical reactions of fuels and the performance of the DCFC unit [17]. The information on the pore size distribution is also crucial particularly for the operation of the DCFC with molten electrolyte because the size of the carbon particles affect their surface area and the possibility to be fully wetted by the electrolyte [17].

All the analyses were conducted for samples of particle size less than 0.2 mm except the porosimetry investigations where the samples of particle sizes of 0.18–0.25 mm were used. The results of the analyses are summarized in Table 1. The carbon content in all the fuels exceeds 80%. The surface area differs significantly—the measured values vary from 0.2 $m^2\ g^{-1}$ (graphite rod) to over 31 $m^2\ g^{-1}$ for carbon black.

The pore size distributions of the fuel samples are shown in Fig. 2. The investigations were determined with the use of mercury porosimeter Poremaster 33. The pore size distribution of the sample is represented as dV/dlog D where V corresponds to the cumulative pore volume and D is the pore diameter. The results indicate that in all cases the majority of the pores for biomass-derived biochars (2–6) are characterized by diameters of roughly 0.1–10 μm. In the case of hard coals (7, 8) and carbon black (1) the pore size distributions were quite narrow and, furthermore, the majority of the pore volume peaks corresponded to the pores less than 0.5 μm. The graphite sample (9) showed two separate peaks at 0.07 μm and 1 μm.

2.2. The DCFC

The schematic diagram of the designed fuel cell is shown in Fig. 3. The cell was manufactured from nickel and nickel alloys. The main cell container (83 mm i.d. and roughly 147 mm high) was manufactured from Nickel® 201. The anode was also made from Nickel® 201, while the cathode was Ni-based Inconel® alloy 600. The anode and cathode were designed as pipes with outside diameters of 19.1 mm and 42 mm, respectively. Both electrodes were subjected to simultaneous oxidation–lithiation process before their implementation into the DCFC. The current and power densities were calculated for the measured anode surface area of 17 cm^2. The anode and cathode were separated in order to prevent any mixing at the gases (CO_2 above the anode and excess air above the

Table 1
Main parameters of the fuels tested (all values are given for a "dry" state).

Fuel sample	Ultimate analysis (wt%)					Ash (wt%)	Volatile matter (wt%)	Higher heating value (MJ kg^{-1})	Surface area (m^2 g^{-1})	Pore volume (cm^3 g^{-1})
	C	H	N	S	O^{diff}					
Graphite rod	97.4	0.6	0.2	0.00	0.10	1.7	1.2	32.35	0.21	0.02
Biochar 1 (apple)	80.3	2.8	1.9	0.00	4.30	10.7	16.8	29.55	6.65	0.25
Biochar 2 (energetic willow)	82.2	2.5	1.3	0.01	5.49	8.5	13.9	29.86	2.68	0.32
Biochar 3 (sunflower husks)	84.1	2.5	2.4	0.03	1.97	9.0	16.1	32.11	3.99	0.20
Biochar 4 (pine)	90.4	2.9	0.6	0.00	3.60	2.5	9.0	33.27	1.52	0.29
Commercial biochar	84.2	3.3	0.5	0.01	9.29	2.7	16.4	29.93	1.14	0.11
Coal 1	70.0	4.5	1.1	1.38	11.52	11.5	36.6	26.74	4.05	0.04
Coal 2	78.5	4.6	1.3	0.89	10.11	4.6	30.4	31.15	6.60	0.04
Carbon black	98.0	1.0	0.4	0.48	0.12	0.0	2.7	33.69	31.34	0.48

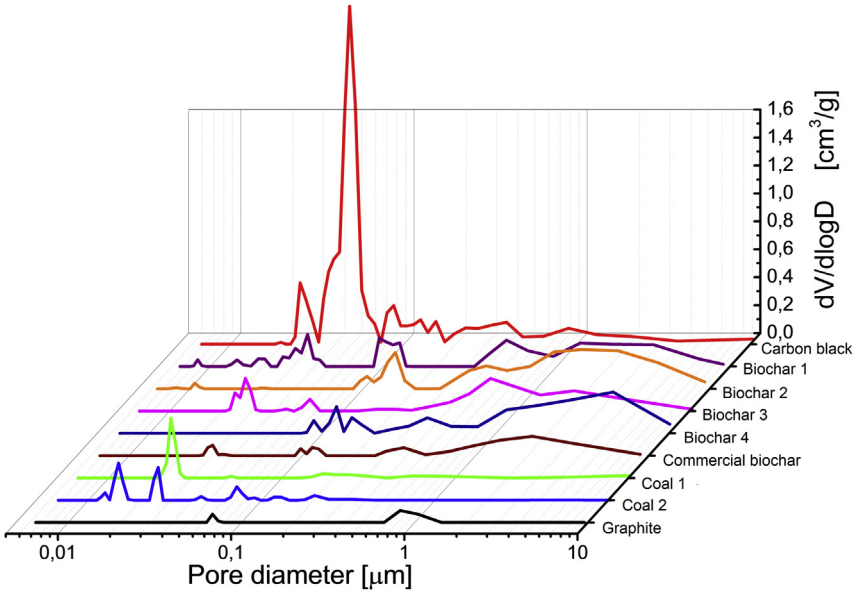

Fig. 2. Pore size distributions of the investigated carbon fuel samples. Measurement technique: mercury porosimetry.

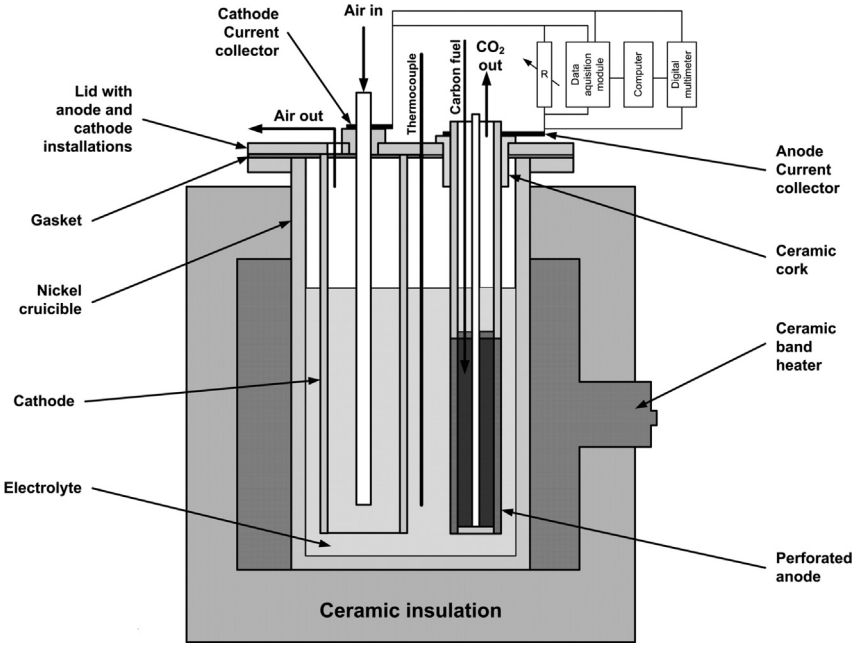

Fig. 3. The outline of the experimental DCFC setup.

cathode). The air was introduced into the cathode pipe where it was contacted with the inner surface of the cathode and then exit to atmosphere. The CO_2 formed at the anode was released to the atmosphere but it could not be contacted with the air flow (see Fig. 3). Additional details of the configuration and the operation of the DCFC were described elsewhere [14,18].

2.3. Test methodology

At the beginning of each test the eutectic mixture of NaOH–LiOH (90–10 mol%) was prepared and then heated up to the desired temperature. After the temperature of 723 K was reached and the electrolyte was completely melted, both cathode and anode were slowly immersed into the electrolyte and the cell data (current, voltage, temperature, etc.) were recorded. The tests were then performed at 723 K. The air to the fuel cell was fed from a compressor (pressure of 0.15 MPa) with controlled flow rate of 0.5 dm^3 min^{-1}. Particle size of fuel samples was in the range of 0.18–0.25 mm.

After each test was finished the heating was turned off and the cell was 'shutdown'. The setup was then cooled down to room temperature and then all its parts were placed in special plastic container filled with roughly 25 dm^3 of deionized water. All the elements were kept there for 3 h in order to get the solidified electrolyte removed. Mechanical stirrer was used to improve the dissolution of the electrolyte. The water-electrolyte mixture was then removed and new 25 dm^3 of deionized water were put into the container. The whole procedure was then repeated. Afterward, the cell elements were removed from the container, cleaned with a soft sponge, and finally again rinsed with deionized water. All the elements were then dried for 2 h in a drier.

3. Results and discussion

3.1. Repeatability of the results

The first stage of the study was carried out to investigate the repeatability of the research results, i.e., to determine whether the data collected during each individual test run are repeatable. The above assumption was confirmed by independent experiments which were carried out at 723 K with the air flow rate of 0.5 dm^3 min^{-1} and for two chosen fuels: coal 1 and commercial biochar (cf. Table 1).

The results for two independent tests are presented in Fig. 4 where a comparison of cell operating characteristics taken at different time intervals in each cell run are shown. The first characteristic was taken after 4 h, the second one after 5 h, and the third one after 6 h of cell operation. All curves are similar in shape and all drop from the maximum voltage of roughly 1.1 V for the current density $i = 0$ mA cm^{-2}) to nearly 0.2 V for $i = 75$ mA cm^{-2}. As indicated by the results the linear middle region of the characteristics confirms that the DCFC operation is controlled by ohmic resistance. In case of commercial biochar (cf. Fig. 4B) the decrease of the voltage at high current densities, roughly 70–80 mA cm^{-2}, is associated with concentration polarization. The maximum power densities for coal were 28.4 mW cm^{-2}, 29.1 mW cm^{-2} and 27.9 mW cm^{-2} for the characteristics No. 1, No. 2 and No. 3, respectively (cf. Fig. 4A). The corresponding maximum power densities for the biochar were 35.1 mW cm^{-2} (characteristic No. 1), 34.5 mW cm^{-2} (characteristic No. 2) and 34.6 mW $cm^{-2}$for the characteristics No. 3 (cf. Fig. 4B). The results indicate very good repeatability of the experimental values and meet the initial authors' assumptions.

The variations of the cell voltage plotted against time for the current I = 0 A are plotted in Fig. 5A and the relationships between

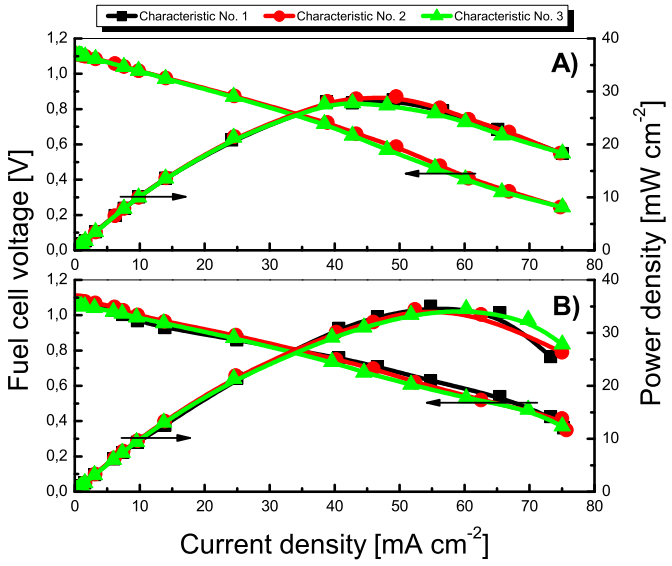

Fig. 4. The comparison of the fuel cell characteristics for some chosen fuels: (A) coal 1, and (B) commercial biochar. Particle size: 0.18–0.25 mm, electrolyte temperature: 723 K, air flow rate: 0.5 dm^3 min^{-1}.

cell voltage, power density, and current density for an example fuel (commercial biochar) are shown in Fig. 5B. The characteristics shown in Fig. 5B were taken after 4 h of cell operation. For all runs the stable voltage level was achieved after roughly a 2 h 'starting' period. The voltage values obtained after 4 h of the DCFC operation were 1.08 V, 1.06 V and 1.08 V for the Run No. 1, 2, and 3, respectively. Similar curves were also obtained for the other tested fuels.

It is worth noting that, compared to other characteristics, the characteristic of Run No. 3 (cf. Fig. 5B) is somewhat lower at the initial current density region but it becomes slightly higher at the end region. The difference may probably be associated with the random distribution and arrangement of fuel particles at the surface of the anode chamber collector. This hypothesis is partially supported by Fig. 6 indicating that despite similar particle size (0.18–0.25 mm) the shape of the fuel particles is quite different, e.g., rectangular, spherical or spindle. The internal resistances (R_i), calculated from the slope of the linear region of each curves in Fig. 5B, are similar. The corresponding values of R_i were 0.52 ± 0.03 Ω (for Run No. 1), 0.48 ± 0.01 Ω (for Run No. 2) and 0.42 ± 0.02 Ω for Run No. 3. The maximum current densities obtained for the runs No. 1, 2 and 3 were 73.1 mA cm^{-2}, 73.3 mA cm^{-2} and 75.2 mA cm^{-2}, respectively, while the corresponding maximum power densities (cf. Fig. 5B) were 34.0 mW cm^{-2}, 35.7 mW cm^{-2} and 35.1 mW cm^{-2}.

The comparison of the results in Figs. 4 and 5 clearly indicates that the fuel cell is run stable and the experimental data values are reproducible and reliable. Some minor differences in the characteristics are probably the result of manual feeding of the fuel into the anode chamber or different geometry and arrangement of the carbon particles in the anode (cf. Fig. 6).

3.2. The open circuit voltage

In a perfect working fuel cell the measured open circuit voltage OCV (i.e., the maximum voltage that could be achieved at the current I = 0 A) should equal to the reversible potential. For the DCFC operated at 700 K the reversible potential, E, can be calculated by dividing the change of the Gibbs' energy for the reaction (4) ($\Delta G = -395.4$ kJ mol^{-1} at 700 K) by the number of electrons

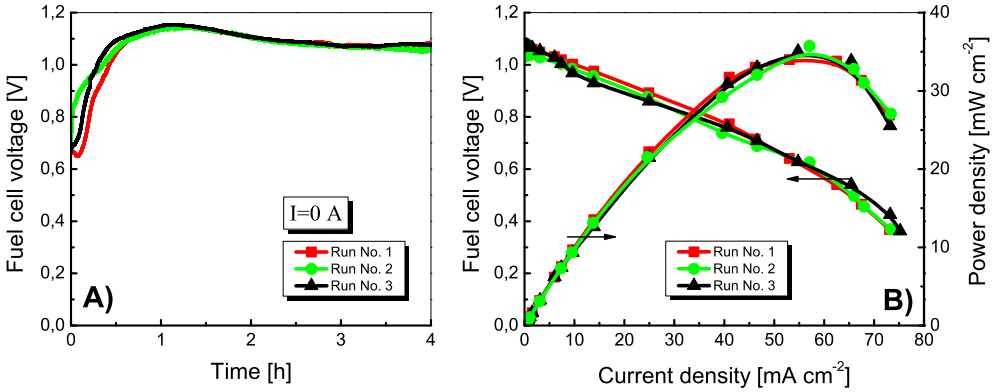

Fig. 5. The variation of the fuel cell voltage vs. time (A) and power–voltage–current density characteristics (B) taken during independent fuel cell runs. Fuel: commercial biochar, particle size: 0.18–0.25 mm, electrolyte temperature: 723 K, air flow rate: 0.5 dm^3 min^{-1}.

transferred in a single run ($n = 4$; as given in Eqs. 2 and 3), and by the Faraday constant ($F = 96485.3$ C mol^{-1}). The value of the reversible potential, calculated according to Eq. (5), is thus 1.025 V.

$$\text{Anode reaction: } C_{(s)} + 4OH^-_{(electrolyte)} \rightarrow CO_{2(g)} + 2H_2O_{(g)} + 4e^- \quad (2)$$

$$\text{Cathode reaction: } 4e^- + O_{2(g)} + 2H_2O_{(g)} \rightarrow 4OH^-_{(electrolyte)} \quad (3)$$

$$\text{Overall reaction: } C_{(s)} + O_{2(g)} \rightarrow CO_{2(g)} \quad (4)$$

$$E = -\Delta G/nF = 1.025\ V \quad (5)$$

The OCV vs. time curves determined during the experiments for various fuels are plotted in Fig. 7. The OCV was measured directly as voltage between the cathode and the anode. The half-cell potential values of the anode and the cathode were not determined in the experiments due to some technical uncertainty associated with the choice of an appropriate reference electrode.

As indicated by the results the OCV is strongly depended on fuel type. For all other cases the cell voltage increased slowly until it reached a stable *plateau* after roughly 2 h and then remained quite stable (see Fig. 7). The only difference was recorded for the fuel 'biochar 4' (i.e., charred pine) for which strong voltage fluctuations after 2 h of continuous cell operation were still measured. The fluctuations might be associated with the origin of the biochar: it was the only fuel that was obtained from forest resin-rich biomass and thus might still contain some impurities or tar-like compounds which could be evolved from the fuel during the test. The differences between the OCV values, particularly at the initial period of roughly 1 h, were probably brought about by gradual wetting of the inner surface of the fuel particles by liquid molten electrolyte. The phenomenon was already discussed by e.g., Cooper and Selman [19] who determined that OCV increase was observed during the gradual wetting of the entire exterior surface of the graphite rod immersed *in* molten carbonate mixture. Later on, the OCV in their experiment reached a certain quasi-steady level value. The authors explained that the phenomenon was associated with the transition of the meniscus between the fuel and the electrolyte from a non-wetting to a wetting one [19]. Similar situation was also observed in this study (cf. Fig 7).

The experimental results of the OCV measured with the use of digital multimeter and data acquisition system after 4 h of cell continuous operation are presented in Table 2. The highest values were recorded for raw coals while the worst results were obtained for graphite rod – probably due to poor surface area and total pore volume of the graphite as shown in Table 1. The OCV values for biomass-derived biochars 1, 2, and 3 (cf. Table 2) are similar, roughly 1 V. It is interesting that the experimental OCV values measured for some fuels (commercial biochar, biochar 3, and both hard coals – see Table 2 and Fig. 7) exceeded the theoretical standard potential of 1.025 V (cf. Eq. (5)). One of the possible reasons may be associated with chemical composition of the fuels and the presence of some impurities that may also be chemically

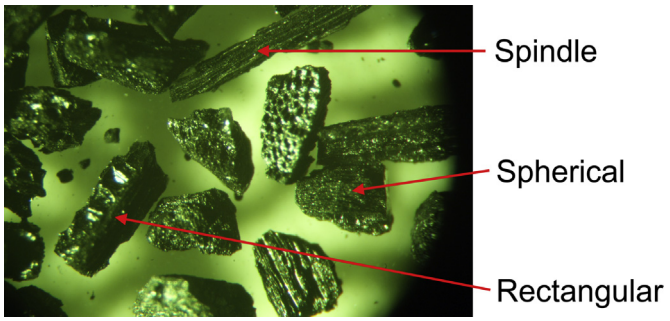

Fig. 6. Some example biochar particles. Fuel: commercial biochar, particle size: 0.18–0.25 mm, magnification: 28×.

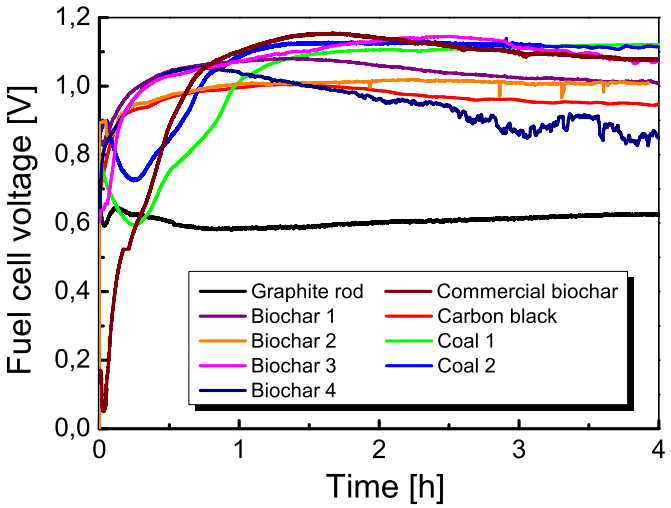

Fig. 7. The DCFC open circuit voltage (at I = 0 A) vs. time for various fuels. Fuel particle size: 0.18–0.25 mm, electrolyte temperature: 723 K, air flow rate: 0.5 dm^3 min^{-1}.

Table 2
Open circuit voltage (OCV) for various fuel samples measured after 4 h of continuous operation of the DCFC.

Fuel sample	Graphite rod	Biochar					Carbon black	Coal 1	Coal 2
		1	2	3	4	Commercial			
OCV [V]	0.6256 ± 0.0008	1.0047 ± 0.0011	1.0090 ± 0.0011	1.0526 ± 0.0008	0.8666 ± 0.0057	1.0749 ± 0.0007	0.9455 ± 0.0004	1.1234 ± 0.0002	1.1196 ± 0.0007

oxidized in the cell. As indicated by the results, the cell fueled with hard coals and chars yielded higher OCV compared to graphite rod and/or carbon black fuels (roughly above 1 V compared to 0.6 V, and 0.95 V, respectively). Similar results were also reported by Hackett G.A et al. [11] who pointed out that the coal-derived fuel rods 'produced' higher OCV (roughly 0.95–1.05 V) compared to the graphite ones (0.7–0.8 V). They concluded that the differences were brought about by the differences of the molecular alignment of carbon in the fuel rods: in the case of coal-derived rod the carbon was more 'easily' accessible for the reaction with OH^- ions (cf. Eqs. 2 and 3) and hence those rods showed a higher electrochemical activity. This assumption has also been supported by some other researchers [5,20–22] who generally agreed that more disordered forms of carbon were usually responsible for higher oxidation reaction rates, higher OCV, and higher current and power densities.

3.3. The effect of fuel type on current density

The fuel cell voltage versus current density is shown in Fig. 8. As indicated by the results shown in Fig. 8 the current–voltage characteristics of the tested DCFC are dominated by ohmic losses (electrolyte, current collectors, and carbon resistivity). The comparison of the polarization curves for the tested fuels indicates no strong effect of the activation polarization. The only exception is the charred pine (biochar 4) for which the activation and concentration polarization are also significant. Biochar 4 was the only fuel for which three regions of polarization were clearly observed. The different behavior of biochar 4 may probably be the result of the presence of some tar-like compounds (e.g., of resin-origin) or other hydrocarbons that were not fully evolved from the biomass fuel during its carbonization.

The maximum current densities are summarized in Fig. 9 for various carbonatious fuels. The measured values were between 28.1 mA $cm^{-2}$and 91.5 mA cm^{-2} and were depended on the fuel type. The most promising results were obtained for hard coals (74.9 mA cm^{-2} and 91.5 mA cm^{-2} for coal 1 and coal 2, respectively), commercial biochar (75.3 mA cm^{-2}) and carbon black (67.0 mA cm^{-2}).

In order to compare the current densities at similar voltage for all the tested fuels, it was decided to present the data for 0.5 V. The corresponding results are also shown in Fig. 9. In the case of charred biomass (biochars 1–4) the current densities at 0.5 V were between 36.0 and 44.6 mA cm^{-2} and were lower than those of the other fuels (55–72.5 mA cm^{-2}). The lowest value was obtained for a graphite rod (5.2 mA cm^{-2}), probably due to the anisotropy of its crystal structure. The results are similar to those of Zecevic S. et al. [10] who reported for 0.5 V the current densities of 50 and 73 mA cm^{-2} for their prototypes MARK IID and MARK IIIA, respectively. They used graphite rod as fuel, molten NaOH as electrolyte and operated their DCFC at 900 K. Similar results to those presented in Fig. 9 were also described in Ref. [11] where the authors reported maximum current densities of 31–53 mA cm^{-2} for the DCFC fueled with coal-derived rods and operated with molten NaOH at 873 K.

3.4. The influence of fuel type on power density

The power density vs. current density curves for various fuels are shown in Fig. 10, while the maximum power densities, determined from the results in Fig. 10, are presented in Fig. 11. The maximum power density made up almost 40 mW cm^{-2}. The lowest value was determined for graphite (5.3 mW cm^{-2}), while the best results were obtained for coal 2 and the commercial biochar. Similar values were obtained for coal 1 and carbon black, 27.9 and 28.4 mW cm^{-2} respectively. The higher current and power densities for coal 2 exceeded those of coal 1 probably due to the higher content of elemental carbon and higher surface area (cf. Table 1). The biochars 1–4 were characterized by quite good values of power densities, roughly between 18.3 mW cm^{-2} and 22.4 mW cm^{-2}. It may be pointed out that contrary to the results for hard coals or carbon black probably the pore-size distribution of the biochars affected their good performance in the DCFC. Those fuels are characterized by larger pores (pore size >0.1 μm, cf. Fig. 1) and thus larger surface of fuel particles could be exposed to better contact with electrolyte molecules. However, the results in Figs. 10 and 11 also indicated that the highest power densities were obtained for the DCFC fueled with hard coals, i.e., fuels containing small pores of sizes <0.1 μm. Those differences may probably be associated with the differences in morphology and structure of individual fuel particles. Similar values of power densities to those shown in Fig. 10 were also obtained by Hackett G.A et al. [11] who reported for coal-derived fuel the maximum power densities of 20–33 mW cm^{-2}. The best results were reported by Zecevic S. et al. [10] who presented the power densities of roughly 57 mW cm^{-2} and 40 mW cm^{-2} for their prototype graphite rod fueled MARK IID and MARK IIIA DCFC setup.

The analysis of the experimental results and their comparison with the data shown in Table 1 indicated that for biochars and coals the maximum power density may also be correlated with fuel oxygen content. This is probably due to the possibility to incorporate oxygen into the surface functional groups that may then increase the reactivity of the carbon matrix [23]. The corresponding relationship for some tested fuels is shown in Fig. 12. The results are very interesting and further investigations are planned by the authors to determine the effect of oxygen-containing functional groups on the performance of the fuel cell.

4. Conclusions

On the basis of the analysis of the information reported and discussed in the present paper the following major conclusions may be formulated:

1. The experimental test results successfully demonstrated the potential of the DCFC to be operated with molten hydroxide electrolyte and also demonstrated the possibility to operate the DCFC with various carbonaceous fuels, some of them of biomass origin.
2. The investigation of the effect of fuel type on the cell performance indicated that the properties and structure of the

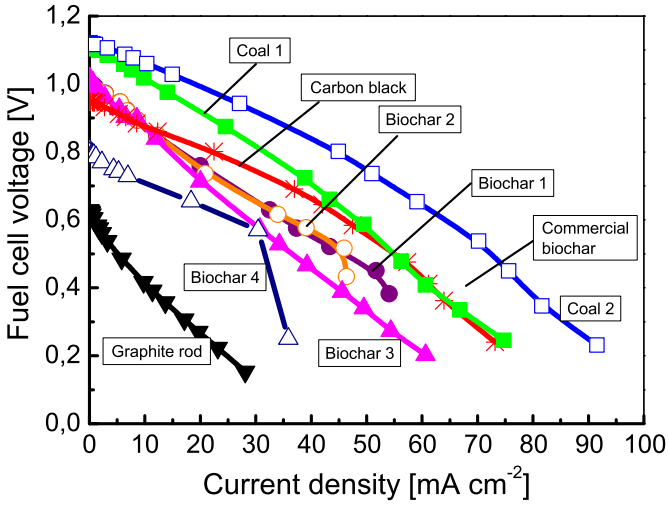

Fig. 8. Fuel cell voltage vs. current density for various fuel types. The DCFC was operated at 723 K with an air flow rate of 0.5 dm^3 min^{-1}. Fuel particle size: 0.18–0.25 mm.

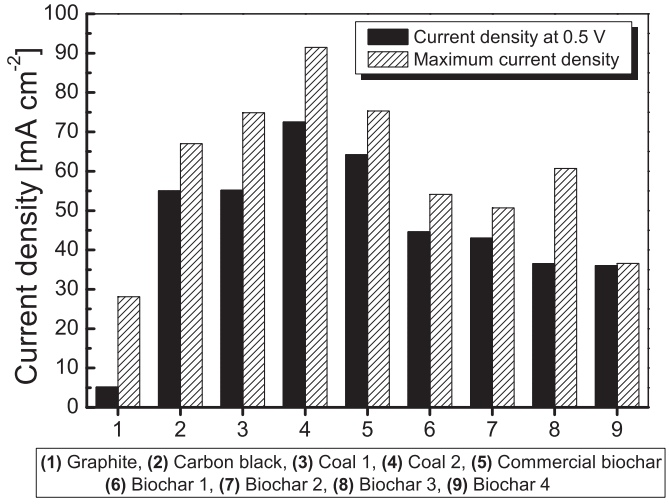

Fig. 9. Summary of the current densities for various carbonaceous fuels.

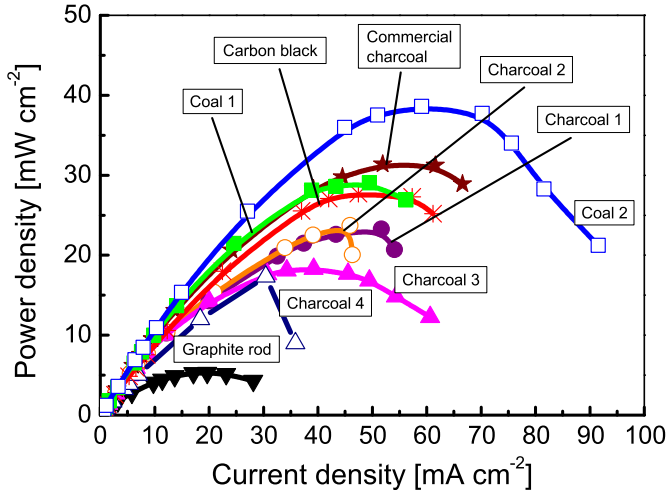

Fig. 10. Power density vs. current density for various fuel types. The DCFC was operated at 723 K, air flow rate 0.5 dm^3 min^{-1}, fuel particle size: 0.18–0.25 mm.

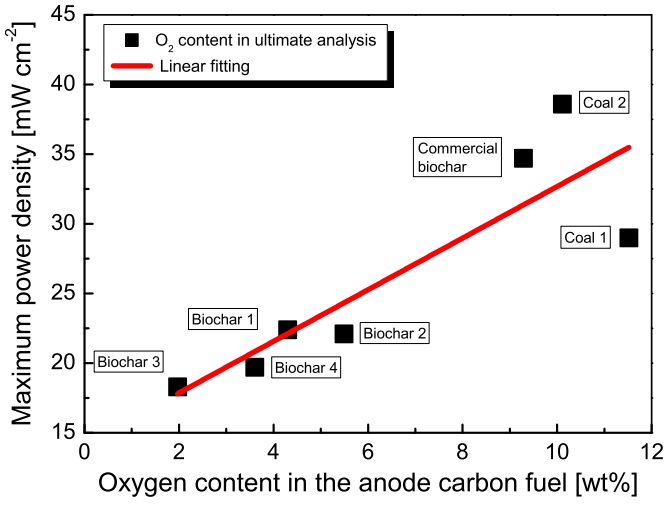

Fig. 12. The relationship between oxygen content in the carbon fuel and the maximum power density.

carbonaceous fuels significantly affected the performance of the fuel cell. It was evident that the 'disordered' carbon was more reactive.

3. From all the investigated fuels the highest current (at 0.5 V) and power densities were determined for hard coal 2, and commercial biochar. The corresponding values were 72.5 mA cm^{-2} and 38.6 mW cm^{-2} for hard coal 2, and 64.2 mA cm^{-2} and 32.8 mW cm^{-2} for the commercial biochar.
4. The current (at 0.5 V) and power densities for biomass-derived biochars were quite promising and made up: 44.6 mA cm^{-2} and 22.4 mW cm^{-2} (biochar 1), 43 mA cm^{-2} and 22.1 mW cm^{-2} (biochar 2), 36.5 mA cm^{-2} and 18.3 mW cm^{-2} (biochar 3) and 36 mA cm^{-2} and 19.7 mW cm^{-2} (biochar 4)
5. The maximum power density, P_{max}, of the investigated carbon fuels was almost 40 mW cm^{-2}. The values of the P_{max} decreased depending on the fuel type in the following order: raw hard coal > commercial biochar > carbon black > laboratory charred biomass > graphite.
6. The experimental results indicated the existence of a correlation between the fuel oxygen content and the maximum measured power density, P_{max}. The correlation is probably associated with the presence of oxygen-containing functional groups in the fuel matrix. The phenomenon requires some further investigations that are currently planned by the authors.

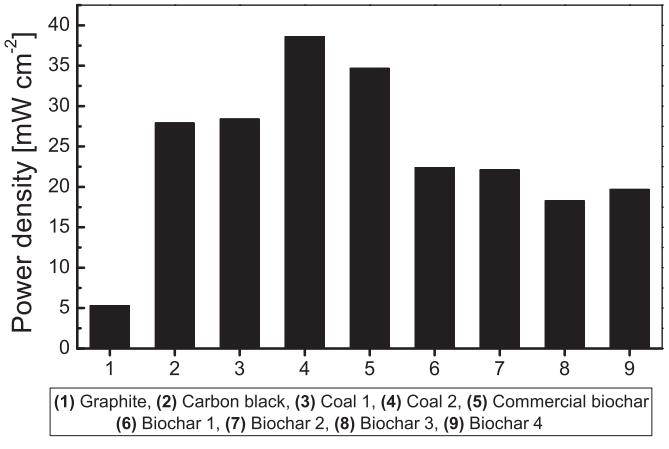

Fig. 11. Comparison of the maximum cell power densities for various fuels.

Acknowledgment

This work has been supported by the Polish Ministry of Education and Science under grant No. N N513 396 736.

One of the authors (A. Kacprzak) is also indebted for the financial support to the DoktoRIS – Scholarship Program for Innovative Silesia, co-financed by the European Union within the framework of the European Social Fund.

References

[1] European Parliament and Council, Directive of the European Parliament and of the Council on the Promotion of Electricity Produced from Renewable Energy Sources in the Internal Electricity Market, 2001. Directive 2001/77/EC – 27 September 2001, Brussels.
[2] Directive on the Promotion of the Use of Energy from Renewable Sources, European Commission, Brussels, 2009.
[3] IEA, Key World Energy Statistics 2012, 2012 (accessed 08.09.13), http://www.iea.org/publications/freepublications/publication/kwes.pdf.
[4] World Coal Association, Coal Facts 2012, 2012 (accessed 06.06.13), http://www.worldcoal.org/bin/pdf/original_pdf_file/coal_facts_2012(06_08_2012).pdf.
[5] Technology Roadmap: High-efficiency Low-emissions Coal-fired Power Generation, Publication of International Energy Agency, 2012. www.iea.org (accessed 06.06.13).
[6] D. Cao, Y. Sun, G. Wang, J. Power Sources 167 (2) (2007) 250–257.
[7] S. Srinivasan, Fuel Cells: From Fundamentals to Applications, Springer, NY, USA, 2006.
[8] S. Giddey, S.P.S. Badwal, A. Kulkarni, C. Munnings, Prog. Energy Combust. Sci. 38 (2012) 360–399.
[9] S. Zecevic, E.M. Patton, P. Parhami, Carbon 42 (2004) 1983–1993.
[10] S. Zecevic, E.M. Patton, P. Parhami, Chem. Eng. Commun. 192 (2005) 1655–1670.
[11] G.A. Hackett, J.W. Zondlo, R. Svensson, J. Power Sources 168 (2007) 111–118.
[12] T. Nunoura, K. Dowaki, C. Fushimi, S. Allen, E. Meszaros, M.J. Antal, Ind. Eng. Chem. Res. 46 (2007) 734–744.
[13] A. Kacprzak, R. Włodarczyk, R. Kobyłecki, M. Ścisłowska, Z. Bis, Fuel cell as part of clean technologies, in: A. Pawłowski, M.R. Dudzińska, L. Pawłowski (Eds.), Environmental Engineering IV, CRC Press, Taylor & Francis Group, London, 2013, ISBN 978-0-415-64338-2, pp. 443–450.
[14] A. Kacprzak, R. Kobyłecki, Z. Bis, J. Power Sources 239 (2013) 409–414.
[15] R. Koby1ecki, Z. Bis, The carbonization of biomass for renewable energy and carbon sink, in: Proc. of the 3rd Int. Conf. on Contemporary Problems of Thermal Engineering, CPOTE 2012, Gliwice, Poland, September 18–20, 2012, ISBN 978-83-61506-13-3, pp. 185–186.
[16] R. Koby1ecki, J. Tchórz, Z. Bis, Densification of biomass energy for large scale Co-combustion, in: Proc. of the 9th Int. Conf. on Circulating Fluidized Beds (CFB-9) in Conjunction with 4th Int. VGB Workshop, Hamburg, Germany, May 13-16, 2008, ISBN 978-3-930400-57-7, pp. 839–843.
[17] S.Y. Ahn, S.Y. Eom, Y.H. Rhie, Y.M. Sung, et al., Appl. Energy 105 (2013) 207–216.
[18] A. Kacprzak, R. Kobyłecki, Z. Bis, Arch. Thermodyn. 32 (3) (2011) 37–47.
[19] J.F. Cooper, R. Selman, ECS Trans. 19 (2009) 15–25.
[20] N.J. Cherepy, R. Krueger, K.J. Fiet, A.F. Jankowski, J.F. Cooper, J. Electrochem. Soc. 152 (1) (2005) A80–A87.
[21] J.F. Cooper, Direct conversion of coal and coal-derived carbon in fuel cells, in: Second International Conference on Fuel Cell Science, Engineering and Technology, ASME, Rochester, NY, June 14–16, 2004.
[22] X. Li, Z. Zhu, R. De Marco, J. Bradley, A. Dicks, J. Power Sources 195 (13) (2010) 4051–4058.
[23] X. Li, Z.H. Zhu, J.L. Chen, R. De Marco, A. Dicks, J. Bradley, et al., J. Power Sources 186 (2009) 1–9.